An Alkaline-Developable, Chemically Amplified, Negative-Type Photosensitive Poly(benzoxazole) Resist Based on Poly(*o*-hydroxy amide), an Active Ester-Type Cross-Linker, and a Photobase Generator

Katsuhisa Mizoguchi, Tomoya Higashihara, and Mitsuru Ueda*

Department of Organic and Polymeric Materials, Graduate School of Science and Engineering, Tokyo Institute of Technology, 2-12-1 O-okayama, Meguro-ku, Tokyo, 152-8552, Japan

Received October 19, 2008; Revised Manuscript Received December 27, 2008

ABSTRACT: An alkaline-developable, chemically amplified, negative-type, photosensitive poly(benzoxazole) (PSPBO) based on poly(*o*-hydroxy amide) (PHA), an active ester-type cross-linker bis(*p*-nitrophenyl) suberoylate (BNPS), and *N*-{[(4,5-dimethoxy-2-nitrobenzyl)oxy]carbonyl}-2,6-dimethylpiperidine (DNCDP) as a photobase generator (PBG) has been successfully developed to avoid corrosion of copper (Cu) circuits in microchips by a photogenerated acid from photoacid generators (PAGs). This resist film consisting of PHA (80 wt %), BNPS (5 wt %) and DNCDP (15 wt %) showed the high sensitivity ($D_{0.5}$) of 78 mJ/cm^2 and good contrast ($\gamma_{0.5}$) of 4.0 when it was exposed to 365 nm UV light (*i*-line), postexposure baked (PEB) at 140 °C for 10 s, and developed with 2.38 wt % tetramethylammonium hydroxide aqueous solution (TMAH (aq)) as an alkaline developer at 25 °C. A fine negative image featuring 6 μm resolution patterns was obtained on a film (thickness: 2.5 μm) exposed to *i*-line by a contact-printed mode, and developed with 2.38 wt % TMAH (aq). The negative image was converted to the corresponding PBO pattern upon heating at 350 °C. Moreover, this resist system formed 9.3 μm thick pattern having 30 μm resolution with 98 mJ/cm^2 exposure. The resulting PSPBO showed high thermal stability, low water absorption, low dielectric and excellent mechanical properties. This new image formulation method is the first example of PSPBO using the PBG, and provides a good and versatile process which avoids corrosion of Cu circuits in microchips.

Introduction

Photosensitive poly(benzoxazole)s (PSPBOs) are widely utilized as protection and insulating layers in manufacturing semiconductors because of their good mechanical properties, low water absorption, and low dielectric constant.[1–3] Moreover, an outstanding advantage of the PSPBO resist system is to simplify the pattern-formation processes, where phenolic hydroxyl groups in PHA as a precursor of PBO provide adequate solubility to an aqueous alkaline developer. Also, capability of development in an aqueous alkaline solution is beneficial for an environmentally benign process. In general, PSPBOs are formulated from PHA with 20 – 30 wt % *o*-diazonaphthoquinone (DNQ) as a photoactive dissolution inhibitor, which is converted into an alkaline-developable indene carboxylic acid as a dissolution promoter to provide a positive image. Meanwhile, the drawback of the PSPBO system using DNQ is photosensitivity, which is low (in the range of 200–400 mJ/cm^2) to obtain a patterned film.[1,4–6] Recently, chemically amplified-type PSPBOs have been reported to improve the photosensitivity, where PHA is combined with a cross-linker or a dissolution inhibitor, and PAG, which generates the sulfonic acid derivatives.[7–12] However, a photogenerated acid from PAG induces corrosion of Cu circuits in microchips. To overcome this problem, a novel photoimage formation system is strongly required for the next generation PSPBO resist systems. The most straightforward approach is to use PBG instead of PAG, and a base-catalyzed esterification of phenol with an active ester compound is a well-known reaction.[13] Therefore, a PSPBO consisting of PHA, an active ester-type cross-linker, and PBG is expected to provide a new photoimage formation. No reports have been published on the formulation of PSPBOs using the PBG.

In this paper, we report an alkaline-developable, negative-type PSPBO based on PHA, BNPS as an active ester-type cross-linker, and DNCDP as a PBG that provides a chemically amplified PSPBO resist system without corrosion of Cu circuits. The patterning process of this PSPBO system is shown in Scheme 1. The PSPBO resist solution is spin-coated on a silicon wafer and prebaked. Then, the film is exposed to the *i*-line through a photomask to produce 2,6-dimethylpiperidine (DMP) from DNCDP.[14–18] Upon PEB treatment of the PSPBO film, DMP catalyzes the esterification of phenolic hydroxyl groups of PHA with BNPS. The dissolution rate of the exposed area to 2.38 wt % TMAH (aq) decreases and a negative image is formed. Finally, the patterned PHA film is transformed into PBO film by thermal treatment. Furthermore, the thermal and mechanical properties, water absorption, and dielectric constant of the resulting PBO film are also reported.

Experimental Section

Materials. The PHA was prepared from 4,4′-(hexafluoroisopropylidene)-bis(*o*-aminophenol) (6FAP) and 4,4′-oxidibenzoyl chloride in the presence of anhydrous lithium chloride in dehydrated *N*-methyl-2-pyrrolidinone (NMP) as described previously.[19] The number- and weight-average molecular weights (M_n and M_w) of PHAs were 9700 and 20 800, respectively. DNCDP was prepared according to the reported procedure.[14] NMP and cyclopentanone were distilled under reduced pressure after stirring over calcium hydride and then stored over 4A molecular sieves. 6FAP, *p*-nitrophenol, benzoyl chloride, suberoyl chloride, 4,4′-oxybis(benzoic acid), lithium chloride, isopropyl alcohol (*i*-PrOH), triethylamine (TEA), dry tetrahydrofuran (THF), and other reagents were obtained commercially and used as received.

Synthesis of Bis(*p*-nitrophenyl) Suberoylate (BNPS). BNPS was prepared by the reaction of suberoyl chloride with *p*-nitrophenol in the presence of TEA in THF. Recrystallization from ethyl acetate/*n*-hexane (1/4 volume ratio) gives a white crystal. The yield was

* To whom correspondence should be addressed. Telephone: +81-3-57342127. Fax: +81-3-57342127. E-mail: ueda.m.ad@m.titech.ac.jp.

Scheme 1. New Negative-Type PSPBO Resist System Obtained by Using a PBG and an Active Ester-Type Cross-Linker
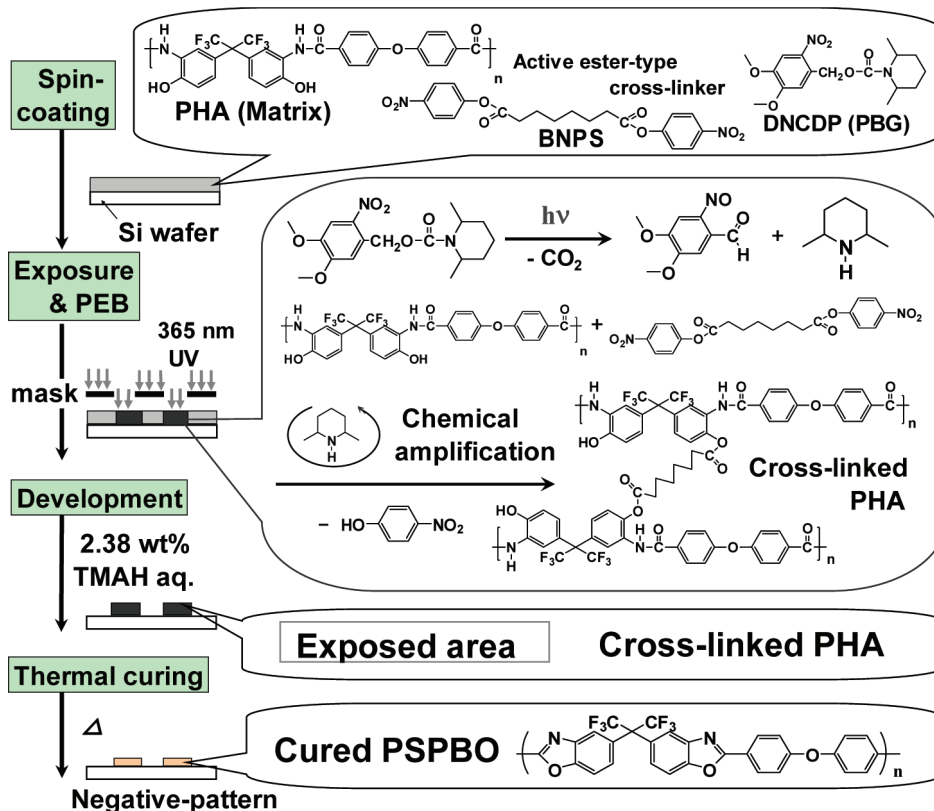
98%. Mp 113−114 °C. (lit.[20] mp 108 °C). Anal. Calcd for $C_{20}H_{20}N_2O_8$: C, 57.69; H, 4.84; N, 6.73. Found: C, 57.46; H, 4.82; N, 6.46.

Model Reaction. PHA (0.050 g, 0.085 mmol), *p*-nitrophenyl benzoate (NPB), (0.041 g, 0.170 mmol), and DNCDP (0.015 g, 0.043 mmol) were dissolved in cyclopentanone (solid content: 33 wt %). The film was prepared by the polymer solution on a glass plate, followed by prebaking at 80 °C for 1 min. Each film was exposed to the *i*-line of 1000 mJ/cm^2, and PEB at 140 °C for a set time. After that, each film on the glass plate was dissolved in acetone (3.0 mL). The solution was evaporated under reduced pressure to obtain a solid. The residue was washed with stirring in the distilled water (30 mL) to remove the eliminated *p*-nitrophenol from NPB after the PEB treatment, filtrated, and dissolved again in acetone (1.0 mL). The polymer solution was poured into toluene (20 mL) to precipitate the *O*-acylated PHA. The precipitate was filtrated, washed with toluene, and vacuum-dried at 110 °C for 6 h. The ^1H NMR spectrum of each *O*-acylated PHA sample was measured in DMSO-d_6 at 40 °C.

Degree of *O*-Acylation of PHA. Peak areas at 8.08−8.30 ppm in ^1H NMR spectra ($I_{Ar\,8.08-8.30}$) due to the *ortho*-protons of the phenyl ester of PHA and 6.95−8.30 ppm ($I_{total\,Ar\,6.95-8.30}$) due to the whole aromatic protons of the *O*-acylation of PHA were measured, and the degree of *O*-acylation was calculated by using the following equation (1):

$$\text{degree of } O\text{-acylation of PHA [\%]} =$$
$$\frac{(I_{Ar\,8.08-8.30[samp]}/I_{total\,Ar\,6.95-8.30[samp]})}{(I_{Ar\,8.08-8.30[O\text{-acylated PHA}]}/I_{total\,Ar\,6.95-8.30[O\text{-acylated PHA}]})} \times 100 \quad (1)$$

Subscripts between brackets followed $I_{Ar\,8.08-8.30}/I_{total\,Ar\,6.95-8.30}$ in eq 1 indicate the intended samples for measurement; e.g., [samp] is the polymer sample treated at each PEB time, followed by precipitation, and drying, and [*O*-acylated PHA] is the fully *O*-acylated PHA, which was prepared by the reaction of PHA with benzoyl chloride in the presence of TEA.

Dissolution Rate. BNPS (5 wt %) and DNCDP (5, 10, and 15 wt %) were added to the PHA solution in cyclopentanone (solid

content: 19.6 wt %). The polymer films were obtained by spin-casting from the solution on silicon wafers. These films were prebaked at 80 °C for 30 s and then exposed to *i*-line followed by PEB at 100−170 °C for 10 s. The exposed films were developed with 2.38 wt % TMAH (aq) and rinsed in water at 25 °C. The dissolution rate (Å/s) of the film was determined from changes in the film thickness before and after the development.

Photosensitivity. The 1.1 μm thick polymer film on a silicon wafer was exposed to the *i*-line followed by PEB at 140 °C for 10 s, and then developed with 2.38 wt % TMAH (aq) for 50 s, and rinsed in water. A characteristic photosensitive curve was obtained by plotting a normalized film thickness as a function of exposure dose (unit: mJ/cm^2).

Preparation of PBO and Cured PSPBO Films for TG, DMA, and Water Absorption Measurement. PSPBO film prepared from PHA/BNPS/DNCDP = 82/3/15 wt % (solid content in cyclopentanone: 36 wt %) was solvent-casted on a glass plate, prebaked at 80 °C for 30 min, exposed by the *i*-line of 500 mJ/cm^2, followed by PEB at 140 °C for 5 min, and curing at 200, 250, 300 °C for each 30 min, and 350 °C for 1 h in the air. On the other hand, PBO film was made from PHA solution, by solvent-casting on a glass plate, curing at 80, 200, 250, 300 °C for each 30 min, and at 350 °C for 1 h in the air.

Water Absorption. Water absorption (WA) was measured by immersing the film into water at 25 °C for 6 h. Then, the film (length, 40 mm; width, 20 mm; thickness, 24−27 μm) was taken out, wiped with a tissue paper, and quickly weighted on a microbalance. Water absorption was calculated from the following equation,

$$WA \text{ (wt \%)} = (W_s - W_d)/W_d \times 100 \quad (2)$$

W_d and W_s stand for the weight of film before and after immersion into water.

Measurements. The infrared spectroscopy (IR) was taken with Horiba FT-210 spectrophotometer. The ^1H NMR spectra were recorded with a BRUKER DPX-300 spectrometer at ^1H 300 MHz. Deuterated chloroform and dimethylsulfoxide were used as a solvent
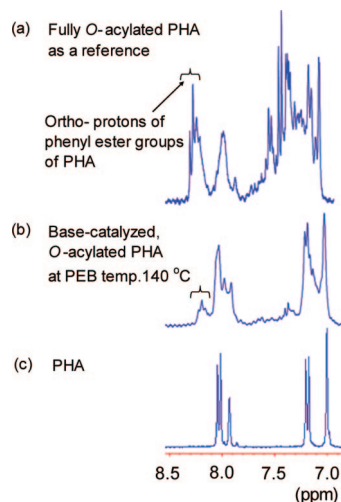
Figure 1. ^{1}H NMR spectra of (a) the fully *O*-acylated PHA with benzoyl chloride, (b) the partly *O*-acylated PHA in the model reaction for the base-catalyzed esterification of PHA with NPB, and (c) PHA.

Figure 2. Degree of *O*-acylation of PHA in the model reaction for the base-catalyzed esterification of PHA with NPB.

Scheme 2. Synthesis of the Fully *O*-Acylated PHA

with tetramethyl silane as an internal standard. Number- and weight-average molecular weights (M_n and M_w) were estimated by a gel permeation chromatograph (GPC) on a Jasco co-2065 Plus system equipped with a polystyrene gel column (TOSOH TSKgel GMH$_{HR}$-M) eluted with THF at a flow rate of 1.0 mL/min calibrated by standard polystyrene samples. Ultraviolet−visible spectroscopy (UV−vis) was performed on a Jasco V-650 spectrophotometer. Thermal analysis was performed on a Seiko EXSTER 6000 at a heating rate of 10 °C/min for thermogravimetry (TG/DTA) under 200 mL/min flow of nitrogen. Dynamic mechanical thermal analysis (DMA) was performed on the PSPBO or thermally cured PSPBO films (30 mm long, 10 mm wide, and 24−27 mm thick) on a Seiko DMS 6300 at a heating rate of 2 °C/min with a load frequency of 1 Hz in air. The glass transition temperatures (T_gs) are determined as the peak temperature of loss module (E'') polts. The film thickness was measured by Veeco Instrument Dektak^3 surface profiler. The scanning electron microscopic image (SEM) was taken by a Technex Laboratory Tiny-SEM 1540 with 5 kV accelerating voltage. Refractive indices of PBO and the cured PSPBO resist films formed on quartz substrates were measured at a wavelength of 1320 nm at room temperature with a Metricon model PC-2000 prism coupler. Using linearly polarized laser light with parallel (TE: transverse electric) and perpendicular (TM: transverse magnetic) polarization to the film plane, the in-plane (n_{TE}) and out-of-plane (n_{TM}) refractive indices. The dielectric constant at 1 MHz frequency was calculated from the following equation as follows, $n_{AV} = [(2n^2_{TE} + n^2_{TM})/3]^{1/2}$, $\epsilon = 1.10 \, n^2_{AV}$, where n_{AV} is an average refractive index.

Results and Discussion

Model Reaction for Base-Catalyzed Esterification (*O*-Acylation) of PHA. To investigate the base-catalyzed esterification of PHA with NPB as an active ester compound in the solid state, polymer films based on PHA, NPB, and DNCDP (molar ratio: 1: 2: 0.5) was exposed to the *i*-line, followed by PEB at 140 °C for each PEB time. After that, each polymer was isolated by precipitation. The progress of *O*-acylation was followed by ^{1}H NMR spectrometry, as shown in Figure 1. The fully *O*-acylated polymer as a reference was prepared by the acylation of PHA with benzoyl chloride (Scheme 2). New signals of protons in the *ortho*-position of the phenyl ester of PHA appear at 8.08−8.30 ppm with the progress of esterification. On the other hand, the ^{1}H NMR spectra of the unexposed polymers after thermal treatment were almost the same as those of PHA. Thus, the esterification proceeds only in the exposed area of the film under this condition. Therefore, the extent of
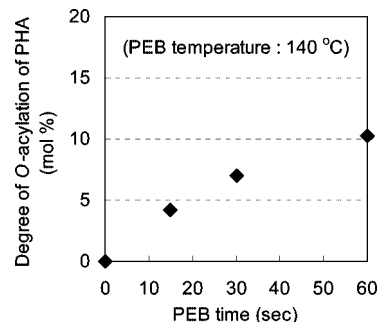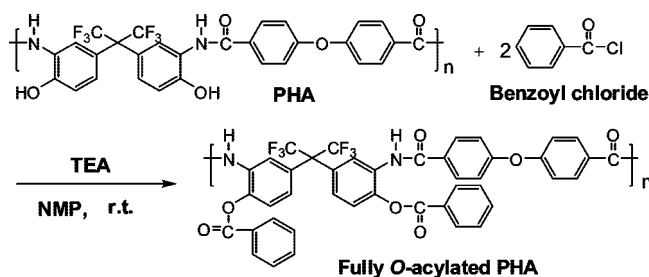
O-acylation of PHA was estimated from eq.(1) in the experimental section, which is based on the integrated ratios of the *ortho*-protons of phenyl ester to whole aromatic protons (6.95−8.30 ppm) of the polymer. The results are shown in Figure 2. The *O*-acylation of PHA proceeds at the PEB temperature, 140 °C, and reaches 10 mol % for 60 s of the PEB time. These behaviors indicate that the esterification of phenolic hydroxyl groups of PHA with NPB occurs by a catalyst DMP photogenerated from PBG after *i*-line irradiation. Therefore, this chemistry was applicable to a novel negative-tone formation in a chemically amplified type of PSPBO resist.

PSPBO Resist Formulation. A cross-linking reaction is very effective to get a high photosensitive polymer because a small percentage of a cross-linking reaction greatly changes the solubility of a polymer. Thus, a base-catalyzed cross-linker, BNPS, was prepared from suberoyl chloride and *p*-nitrophenol in the presence of TEA in THF in quantitative yield.[20] BNPS shows a good solubility in a wide variety of organic solvents due to a flexible aliphatic spacer. In addition, a clearly transparent film can be obtained by spin-coating on a silicon wafer from a solution of PHA and BNPS in cyclopentanone. The UV−vis spectrum of BNPS in chloroform indicates no absorption over ca. 320 nm, which means that BNPS does not prevent the photobase generation from DNCDP from having a strong absorption centered at ca. 340 nm, as shown in Figure 3. A cross-linker should be stable during PEB treatment in the temperature range of about 100−170 °C. Thus, the thermal stability of BNPS was evaluated by TG. The thermal decomposition (1 wt % weight loss) temperature of BNPS at 273 °C indicates its adequate thermal stability.

DNCDP is a thermally stable PBG, and the thermal decomposition temperature is around 200 °C (1 and 5 wt % weight loss temperatures $T_{d1\%} = 197$ and $T_{d5\%} = 222$ °C under nitrogen, respectively).[16] Accordingly, a PSPBO resist-varnish was formulated by mixing PHA with BNPS and DNCDP in cyclopentanone.

Lithographic Evaluation. Preliminary optimization studies of processing conditions and composition ratios of BNPS and DNCDP to PHA for formulation of PSPBO were conducted.
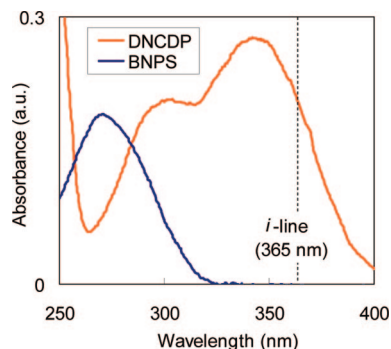
Figure 3. UV−vis spectra of DNCDP (1.4×10^{-5} mol/L) and BNPS (4.3×10^{-5} mol/L) in chloroform.
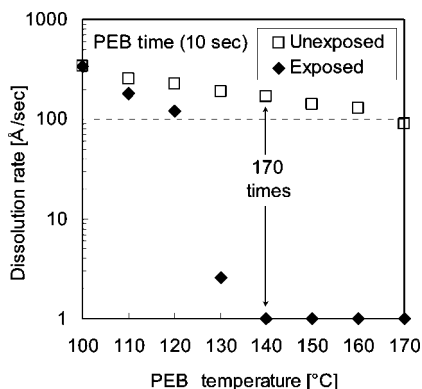

Figure 4. Effect of PEB temperature on the dissolution rate for the PSPBO films in the exposed and unexposed areas.

The films (PHA/BNPS/DNCDP: 80/5/15 wt %, film thickness: 1.1 μm) were obtained by spin-casting the solution of PHA containing BNPS and DNCDP on a silicon wafer and, then, prebaking at 80 °C for 30 s in air. This photosensitive polymer film was irradiated with the *i*-line of 300 mJ/cm^2, PEB at a set temperature, and developed with 2.38 wt % TMAH (aq) at 25 °C. The dissolution rate was calculated by measuring the change of the film thickness before and after development.

The PEB temperature is crucial for the chemically amplified resist system because the diffusion of the base generated from PBG after *i*-line exposure in the film is a very important key factor. First, the effect of PEB temperature on the dissolution rate of the exposed and unexposed areas of the film was studied. The results are shown in Figure 4. The PEB temperatures above 130 °C give a high dissolution contrast (DC) between the unexposed and exposed areas probably because of high diffusion of the photogenerated DMP. As the melting points of DNCDP and BNPS are at 139 and 114 °C, respectively, both additives could work more effectively as platicizers of the films by PEB treatment above 130 °C.

Next, the effect of PEB time on the dissolution rate at 140 °C was studied, the results are shown in Figure 5. The short PEB time is sufficient to get a large DC. This result is also explained by the above discussion.

Finally, the effect of DNCDP loading on the dissolution rate of the polymer films was investigated with 5 wt % BNPS loading at 140 °C for 10 s (Figure 6). The dissolution rate in the exposed area decreases with increasing DNCDP loading and the DC between the exposed and unexposed areas reaches 170-fold in the presence of 15 wt % DNCDP. The need for large DNCDP loading is due to the low quantum yield of DNCDP.[18]

On the basis of these preliminary optimizations, the PSPBO resist system consisting of PHA (80 wt %), BNPS (5 wt %), and DNCDP (15 wt %) was formulated. The photosensitivity curve of a resist film with 1.1 μm thick in the case of PEB
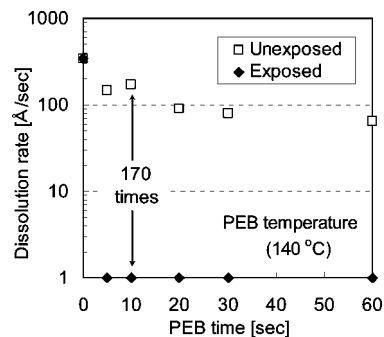

Figure 5. Effect of PEB time on the dissolution rate for the PSPBO films in the exposed and unexposed areas.
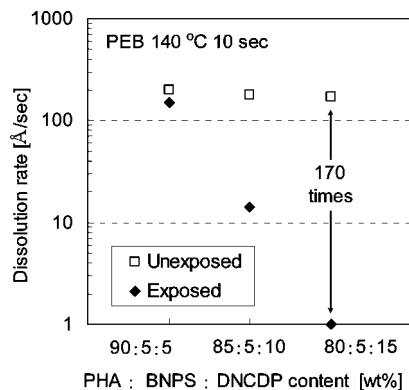

Figure 6. Effect of DNCDP loading on PSPBO (BNPS: 5 wt %) resist on the dissolution rate for the PSPBO films in the exposed and unexposed areas.
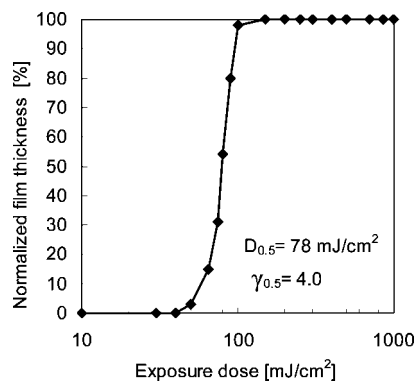

Figure 7. Characteristic photosensitive curve of the PSPBO resist system. $D_{0.5}$ is the sensitivity, and $\gamma_{0.5}$ is the contrast.

treatment at 140 °C for 10 s is shown in Figure 7. This PSPBO resist has excellent sensitivity ($D_{0.5}$) of 78 mJ/cm^2 and good contrast ($\gamma_{0.5}$) of 4.0 with the *i*-line. These findings indicate that the esterification of phenolic hydroxyl groups of PHA with BNPS catalyzed by the photogenerated base is an effective reaction for a negative-type photoimage formation.

Image Formation. Figure 8 depicts an SEM image of a contact-printed pattern obtained with 2.5 μm thick film exposed with the *i*-line of 150 mJ/cm^2, PEB at 140 °C for 10 s, developed with 2.38 wt % TMAH (aq) for 98 s at 25 °C. A clearly negative-tone image with 6 μm resolution was obtained. This negative pattern was successfully converted to the PBO pattern by curing at 350 °C for 1 h (Figure 9). The film became 1.8 μm thick due to cyclization involving the elimination of H$_2$O and the decomposition of unreacted additives such as BNPS and DNCDP. The formation of PBO was confirmed by the IR spectrum, in which the characteristic oxazole ring absorption
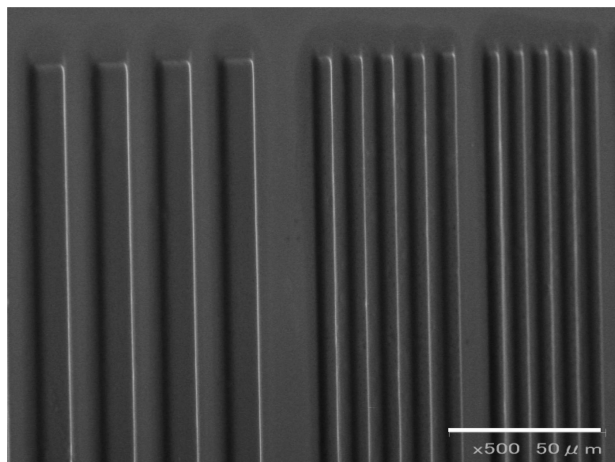
Figure 8. SEM image of the negative-pattern 2.5 μm thick film (PHA/BNPS/DNCDP: 80/5/15 wt %). The lithographic condition was as follows: 22.2 wt % solid content solution in cyclopentanone was spin-coated, prebaked at 80 °C for 30 s, exposed to 150 mJ/cm^2 of *i*-line, PEB at 140 °C for 10 s, and developed with 2.38 wt % TMAH (aq) for 98 s at 25 °C (film thickness before and after development: 2.5 μm).
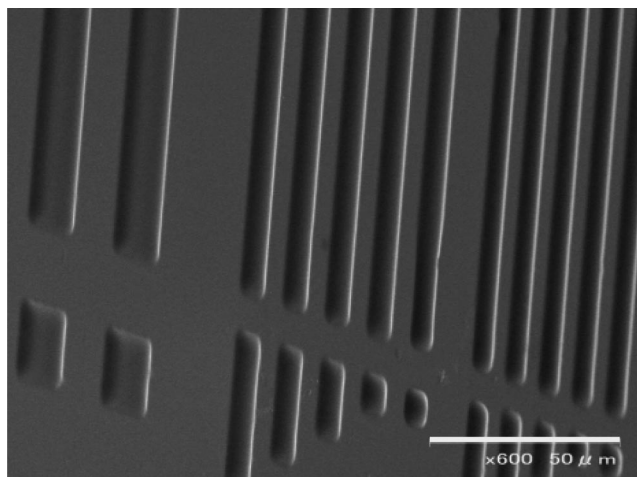

Figure 9. SEM image of the negative-pattern cured at 350 °C for 1 h (film thickness: 1.8 μm).

appeared at 1049 cm^{-1} and the absorptions due to carbonyl groups at 1650 cm^{-1} disappears (Figure 10). The resist system was applied to produce a thicker pattern. A 4 μm resolution image was made in 9.3 μm thick film by PEB at 170 °C for 10 s after exposure to 375 mJ/cm^2 of *i*-line (Figure 11). The exposure doses can be decreased to 98 mJ/cm^2 by increasing BNPS loading from 5 to 7 wt %. The resulting image is also depicted in Figure 12. In the case of the thick film, *i*-PrOH was added in the developer TMAH (aq) not only to dissolve easily the unexposed area in the film but also to suppress the swelling of the exposed area in the film. Adequate resolution and edge sharpness can be seen clearly.

Thermal and Mechanical Properties of Cured PSPBO film. The thermal and mechanical properties of PBO and cured PSPBO were examined by TGA and DMA, and their thermal behavior data are summarized in Table 1. The 10 wt % weight losses of PBO and cured PSPBO were 537 and 529 °C, respectively. Thus, the cured PSPBO exhibits high thermal stability, because the cyclization reaction to PBO and removal of the additives were mainly completed by thermal treatment.

Figure 13 shows the DMA curves of PBO and cured PSPBO films prepared under the same conditions for TG analysis, which
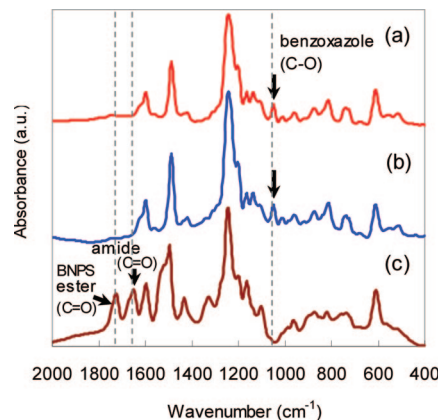

Figure 10. FT-IR spectra of polymer films from PHA on silicon wafers (a) The fully cured PBO film baked at 350 °C for 1 h (b) The fully cured PSPBO film, prebaked at 80 °C for 30 s, exposed to *i*-line of 150 mJ/cm^2, PEB at 140 °C for 10 s, cured at 350 °C for 1 h. (c) The PSPBO resist film after prebaking at 80 °C for 30 s.

was measured at a loading frequency of 1 Hz. The initial storage moduli (E') of PBO and cured PSPBO at ca. 50 °C are 1.4 and 3.5 GPa, and their loss moduli (E'') at the same temperature are 135 and 290 MPa, respectively. Thereby, the cured PSPBO possessed better mechanical properties than PBO due to cross-linkages. The T_g of PBO, determined from the peak temperature of the E'' plots, is observed at 322 °C, whereas the T_g of cured PSPBO can not be detected clearly up to ca. 400 °C due to the cross-linkages between polymer chains. Therefore, the increased T_g of cured PSPBO is one of noteworthy advantages for the permanently embedded resist in microchips, which requires high T_g, like solider resists.

Water Absorption. One of the characteristics of PBOs, compared to polyimides, is relatively low water absorption that maintains a low dielectric constant due to containing no carbonyl groups. The water absorption of PBO and cured PSPBO films at 350 °C is summarized in Table 1. Cured PSPBO film shows low water absorption (less than 0.05%), the same as PBO film.

Dielectric Constant of PSPBO. One of the characteristics of PBO is a low dielectric constant.[21−23] The ϵ values of polymer films around 1 MHz can be calculated from the refractive index (n_{AV}) of the film according to a modified Maxwell's equation, $\epsilon = 1.10 \, n_{AV}^2$. The films of polymers on quartz plates were prepared by spin-coating from their cyclopentanone solution, and then these were prebaked at 80 °C for 30 s in air. Table 2 summarizes the refractive indices and the optically estimated dielectric constant of fully cured PBO film by elevated thermal curing up to 350 °C and the cured PSPBO resist film, which was exposed to 150 mJ/cm^2, PEB at 140 °C for 3 min, cured at 200, 250, 300 °C for 30 min each and finally treated at 350 °C for 1 h in air. The average refractive indices (n_{AV}) of the PBO and cured PSPBO films were determined as 1.5934 and 1.5983, respectively, which were translated into the same ϵ values (2.79). The incorporation of BNPS and DNCDP into PSPBO resist formation did not affect the ϵ value at all, because BNPS, DNCDP and their degradation products which remained after development could be mostly removed by high thermal treatment.

Corrosion Test for Cu-Coated Silicone Wafer. To investigate the corrosion of Cu, PHA films (thickness: 2−3 μm) containing 10 wt % [(5-propylsulfonyloxyimino-5*H*-thiophene-2-ylidene)-(2-methylphenyl)acetonitrile (PTMA)][12] or DNCDP on Cu-coated silicon wafers were exposed to *i*-line of 1000 mJ/cm^2 and placed under a pressurized (2 atm) and relative humidity of 100% for 100 h as an acceleration test. Photographs of the test samples after the acceleration corrosion test are shown in
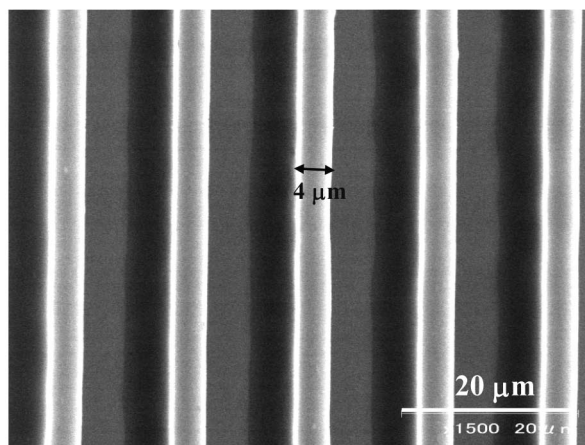
(a)
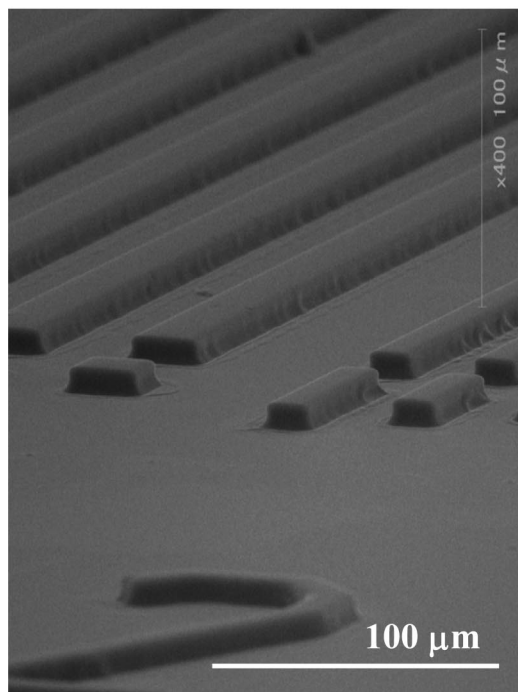
(b)

Figure 11. SEM image of the negative-patterned 9.3 μm thick film (PHA/BNPS/DNCDP: 82/3/15 wt %). (a) 20 and 30 μm resolution pattern (b) 4 μm resolution pattern. (The lithographic condition was as follows; 36 wt % solid content solution in cyclopentanone was spin-coated, prebaked at 80 °C for 60 s, exposed to 375 mJ/cm^2 of *i*-line, PEB at 170 °C for 10 s, developed with 2.38 wt % TMAH (aq) for 240 s, rinsed in water and 2.38 wt % TMAH (aq) containg 5 wt % *i*-PrOH for 160 s at 25 °C, and rinsed again. Film thickness before and after development: 9.3 μm).
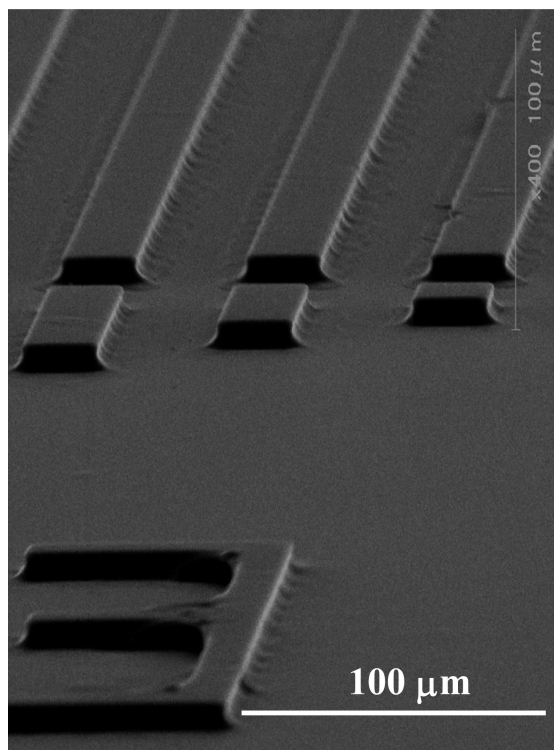

Figure 12. SEM image of the negative-patterned 9.3 μm thick film (30 μm resolution patterned film: PHA/BNPS/DNCDP: 78/7/15 wt %). The lithographic condition was as follows; 36 wt % solid content solution in cyclopentanone was spin-coated, prebaked at 80 °C for 60 s, exposed to 98 mJ/cm^2 of *i*-line, PEB at 170 °C for 15 s, developed with 2.38 wt % TMAH (aq) for 240 s, rinsed in water and 2.38 wt % TMAH (aq) containing 5 wt % *i*-PrOH for 160 s at 25 °C, and rinsed again (film thickness before and after development: 9.3 μm).

Table 1. Thermal Properties and Water Absorption of PBO and Cured PSPBO Films

polymer films	thickness (μm)	T_g (°C)[a]	$T_{d5\%}$ (°C)[b]	$T_{d10\%}$ (°C)[c]	WA (wt %)
PBO	24	322	499	537	<0.05
cured PSPBO	27	not detected	485	529	<0.05

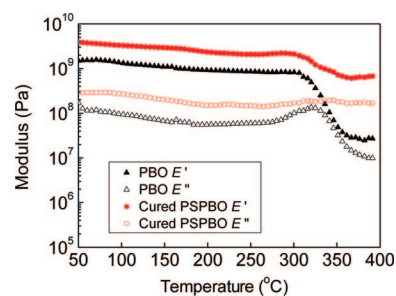[a] Measured by E'' of DMA. [b] Measured by TG. [c] Measured by TG.

Figure 13. DMA curves (storage modulus E' and loss modulus E'', 1 Hz, 2 °C/min, in air) of PBO and cured PSPBO films.

Table 2. Refractive Indices and Dielectric Constants of PBO and Cured PSPBO Films

polymer films	d (μm)[a]	n_{TE}[b]	n_{TM}[c]	n_{AV}[d]	ϵ[e]
PBO	5.8	1.5934	1.5933	1.5934	2.79
cured PSPBO	5.4	1.5983	1.5982	1.5983	2.79

[a] Film thickness. [b] In-plane refractive indices. [c] Out-of-plane refractive indices. [d] Average refractive indices; $n_{AV} = [(2 n^2_{TE} + n^2_{TM})/3]^{1/2}$. [e] Optically estimated dielectric constant; $\epsilon = 1.10\, n^2_{AV}$.

Figure 14. Thereby, only in case of PAG, Cu corrosion of the Cu-coated surface was observed judging from the disappearance of the metallic brilliance. This corrosion is attributed to the diffusion of photogenerated propanesulfonic acids in the polymer

Figure 14. Photograph of their corrosion-tested samples: (a) PHA polymer film with 10 wt % PTMA as PAG on the 0.3 μm Cu-coated silicon wafer; (b) PHA polymer film with 10 wt % DNCDP as PBG on the 0.3 μm Cu-coated silicon wafer.

films. In contrast, photogenerated DMP from PBG does not affect corrosion at all. These results clearly indicate that the new resist formulation method using DNCDP and BNPS is very effective to remedy the corrosion problem of Cu circuits in microchips.

Conclusions

An alkaline-developable, chemically amplified, negative-type PSPBO resist consisting of PHA, an active ester-type cross-linker (BNPS), and DNCDP as PBG was very effective to remedy the corrosion problem of Cu circuits by the acids generated from PAG. This resist system also showed the high sensitivity ($D_{0.5}$) of 78 mJ/cm^2 and good contrast ($\gamma_{0.5}$) of 4.0. After the optimization of photolithographic processes, a clear negative-image pattern with 6 μm resolution was obtained in 2.5 μm thin film. Moreover, this resist system formed a 9.3 μm thick pattern with 30 μm resolution 98 mJ/cm^2 exposure. This is the first example of PSPBO using the PBG, and this new

image formulation method provides a good and versatile process which avoids corrosion of Cu circuits in microchips.

References and Notes

(1) Khanna, D. N.; Mueller, W. H. *Polym. Eng. Sci.* **1989**, *29*, 954–959.
(2) Rubner, R. *Adv. Mater.* **1990**, *2*, 452–457.
(3) Yamaoka, T.; Nakajima, N.; Koseki, K.; Murayama, Y. *J. Polym. Sci., Part A: Polym. Chem.* **1990**, *28*, 2517–2532.
(4) Ebara, K.; Shibasaki, Y.; Ueda, M. *Polymer* **2003**, *44*, 333–339.
(5) Koshiba, M.; Murata, M.; Harita, Y. *Polym. Eng. Sci.* **1989**, *29*, 916–919.
(6) Ueda, M.; Ebara, K.; Shibasaki, Y. *J. Photopolym. Sci. Technol.* **2003**, *16*, 237–242.
(7) Fukukawa, K.; Shbasaki, Y.; Ueda, M. *Macromolecules* **2004**, *37*, 8256–8261.
(8) Fukukawa, K.; Ueda, M. *Polym. J.* **2006**, *38*, 405–418.
(9) Ogura, T.; Yamaguchi, K.; Shbasaki, Y.; Ueda, M. *Polym. J.* **2007**, *39*, 245–251.
(10) Toyokawa, F.; Fukukawa, K.; Shibasaki, Y.; Ando, S.; Ueda, M. *J. Polym. Sci., Part A: Polym. Chem.* **2005**, *43*, 2527–2535.
(11) Naito, K.; Yamaoka, T.; Umemura, A. *Chem. Lett.* **1991**, *38*, 1869–1872.
(12) Asakura, T.; Yamato, H.; Ohwa, M. *J. Photopolym. Sci. Technol.* **2000**, *20*, 223–230.
(13) Os'kina, A. I.; Vlasov, V. M. *Russ. J. Org. Chem.* **2006**, *42*, 865–872.
(14) Mochizuki, A.; Teranishi, T.; Ueda, M. *Macromolecules* **1995**, *28*, 365–369.
(15) Fukukawa, K.; Shbasaki, Y.; Ueda, M. *Polym. Adv. Technol.* **2006**, *17*, 131–136.
(16) Mizoguchi, K.; Shibasaki, Y.; Ueda, M. *J. Photopolym. Sci. Technol.* **2007**, *20*, 181–186.
(17) Frechét, J. M.; Cameron, F. J. *J. Am. Chem. Soc.* **1991**, *11*, 4303–4313.
(18) Blanc, A.; Bochet, G. C. *Org. Lett.* **2007**, *9*, 2649–2651.
(19) Seino, H.; Iguchi, K.; Haba, O.; Oba, Y.; Ueda, M. *Polym. J.* **1999**, *31*, 822–827.
(20) Steinhauser, N.; Muelhaupt, R. *Macromol. Chem. Phys.* **1994**, *195*, 3199–3211.
(21) Fukukawa, K.; Shibasaki, Y.; Ueda, M. *Macromolecules* **2006**, *39*, 2100–2106.
(22) Tsuchiya, K.; Shibasaki, Y.; Ueda, M. *Polym. J.* **2007**, *5*, 442–447.
(23) Fukukawa, K.; Shbasaki, Y.; Ueda, M. *Polym. J.* **2004**, *36*, 489–494.